An *Ab Initio* Modeling Study on a Modeled Hydrated Polymer Electrolyte Membrane, Sulfonated Polyethersulfone (SPES)

Yoong-Kee Choe,*,† Eiji Tsuchida,† Tamio Ikeshoji,† Akihiro Ohira,‡ and Koh Kidena‡

Research Institute for Computational Sciences (RICS), National Institute of Advanced Industrial Science and Technology (AIST), Centeral-2, Umezono 1-1-1, Tsukuba 305-8578, Japan, and Polymer Electrolyte Fuel Cell Cutting-Edge Research Center (FC-Cubic), National Institute of Advanced Industrial Science and Technology (AIST), 2-41-6 Aomi, Koto-ku, Tokyo 135-0064, Japan

Received: July 17, 2009; Revised Manuscript Received: January 12, 2010

The nature of proton dynamics as well as a pendant side chain's ability for proton dissociation and capture in low-hydration sulfonated polyethersulfone (SPES) ($\lambda = 2, 4$) have been studied theoretically by means of quantum chemical calculations and first-principles molecular dynamics simulations. A detailed comparison of results on SPES with those on Nafion has been made. It is found that the sulfonic groups of Nafion tend to dissociate protons more easily than do those of SPES. Hydration by four water molecules allows the dissociation of a proton from the sulfonic groups in both SPES and Nafion. The results of the first-principles MD simulations on SPES show that the nature of proton transfer kinetics for both hydration levels is very similar. Compared with low-hydration Nafion, however, hydration around the sulfonic groups in SPES is not sufficient to fully dissociate protons from the sulfonic groups, which results from the fact that some of the water molecules participate in hydrating SO_2 groups in SPES rather than SO_3^-. Such a feature affects the performance of SPES under low-hydration conditions.

I. Introduction

Polymer electrolyte membrane fuel cells (PEFCs) currently attract a considerable amount of interest because of their potential applications in portable and stationary systems.[1−3] An ionomeric polymer membrane whose role is to facilitate proton conduction and to separate the anode and the cathode is an important component of PEFCs because proton conduction strongly affects the performance of PEFCs. Perfluorinated membranes such as Nafion are widely used in PEFCs because of their excellent mechanical and chemical stability, as well as their good proton conductivity.[4] However, their intrinsic shortcomings, such as high production cost, high methanol permeability, and low operating temperature (<80 °C), have prompted development of novel polymer electrolyte membranes (PEMs) with the aim of achieving properties superior to the perfluorinated membranes in performance while at the same time reducing the overall production cost.[5] PEMs based on hydrocarbons are being extensively studied as alternatives to perfluorinated membranes because they can be easily synthesized by sulfonating existing plastic materials such as polystyrene, that are low in cost and commercially available.[6−13]

In general, hydrocarbon PEMs exhibit proton conductivity comparable to that of Nafion only when the membranes contain a very large number of sulfonic groups,[14,15] which leads to high water uptake and results in poor mechanical properties. It has also been reported that hydrocarbon-based membranes composed of a random copolymer system are less hydrophobic and the sulfonic acid functional groups are less acidic than those of perfluorinated PEMs, which gives rise to poor hydrophobic/hydrophilic phase separation in comparison with that of perfluorinated PEMs such as Nafion.[13,16] The strong acidic nature of Nafion has been attributed to fluorinated backbone, sulfonic acid groups, and the stabilizing effect of the polymer matrix.[17] Indeed, it has been reported that the pK_a value of a sulfonated polyaryl membrane is ~ -1 while its value is ~ -6 in the case of Nafion.[13] Consequently, the proton conductivity of hydrocarbon PEMs is generally lower than that of Nafion when the water content is low, which means that, to obtain proton conductivity comparable to that of Nafion, hydrocarbon PEMs require a high sulfonation level, resulting in a high degree of water uptake. Achievement of good proton conductivity with a low hydration level or with a no-water environment is considered one of the keys for further progress in PEFCs,[18] because water management in water-swollen membranes requires considerable effort.[19] Hence, improvement in the proton conductivity of hydrocarbon PEMs at low hydration levels is an important issue for them to replace Nafion in its position as the best choice for PEFCs. Various strategies for that purpose, such as the introduction of inorganic fillers, are found in the literature.[20] For a rational design strategy, in-depth understanding on the molecular level origin of proton conduction at low hydration levels is necessary. Proton conduction is known to be influenced by membrane morphology, proton dissociation from the acidic functional groups, the nature of proton transport, and hydrogen-bond network.[20,21] As mentioned, it is believed that the sulfonic functional groups in the hydrocarbon PEMs are less acidic. Therefore, it is natural to conjecture that such a difference in the acidity of the sulfonic groups may contribute, to some extent, to the difference in the proton conductivity between hydrocarbon PEMs and Nafion. Moreover, the proton dynamics related to the pendant side chain's ability for proton dissociation and capture need to be investigated to understand the molecular-level origin of proton transport at a low hydration level.[22]

As demonstrated by a series of first-principles molecular simulation (MD) studies on proton transport in water,[23−26]

* Corresponding author. E-mail: yoongkee-choe@aist.go.jp.
† Research Institute for Computational Sciences (RICS).
‡ Polymer Electrolyte Fuel Cell Cutting-Edge Research Center (FC-Cubic).

10.1021/jp906757s
Published on Web 02/02/2010

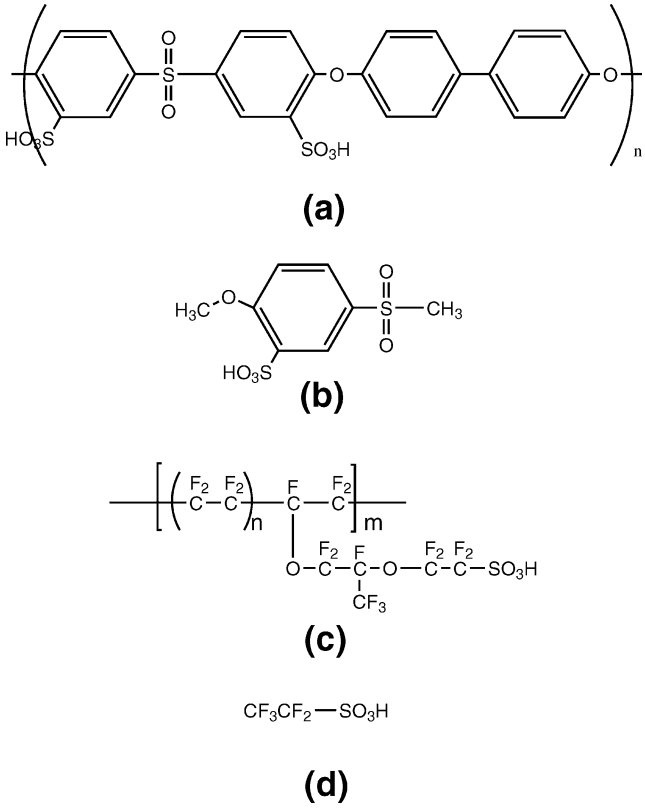

Figure 1. Molecular structure of SPES, Nafion, and their model systems used for microsolvation calculations: (a) SPES; (b) model SPES; (c) Nafion; (d) model Nafion.

atomistic details on proton transport can be elucidated, to a large extent, with the aid of computational modeling. While there have been extensive modeling studies on proton dynamics and transport in PEMs, such studies focus mainly on perfluorinated PEMs.[27−36] As far as we are able to discern, the nature of proton dynamics in hydrocarbon PEMs, which may be beneficial to the clarification of the proton dynamics and transport in hydrocarbon PEMs, has not been investigated theoretically.

In the present study, we report results of computational modeling studies on one of the hydrocarbon PEMs, sulfonated polyethersulfone (SPES). SPES has various attractive features, such as low cost, easy preparation, and controllable composition.[15,37] We investigated the pendant side chain's ability for proton capture and dissociation, as well as dynamical aspects of proton transfer. The former aspect was investigated by means of standard electronic structure calculations for microsolvated clusters of model PEMs employing density functional theory in conjunction with Gaussian basis sets. The latter aspect was explored through first-principles MD simulations employing an adaptive finite-element basis and periodic boundary conditions, a technique that has been successfully applied to molecular liquid and aqueous sulfuric acid solutions,[38−41] as well as PEMs.[42,43] Because of the significance of the proton conductivity of the low-hydration membrane, in the present contribution, we focus on proton dynamics occurring in low-hydration SPES.

II. Computations

A. Quantum Chemical Calculations. The basic ionomer structures of SPES and Nafion are shown in Figure 1. As suggested by Paddison et al., microsolvation of simple model compounds of PEMs is a good and appropriate representation of the state of the membrane under low-hydration conditions.[44−49]

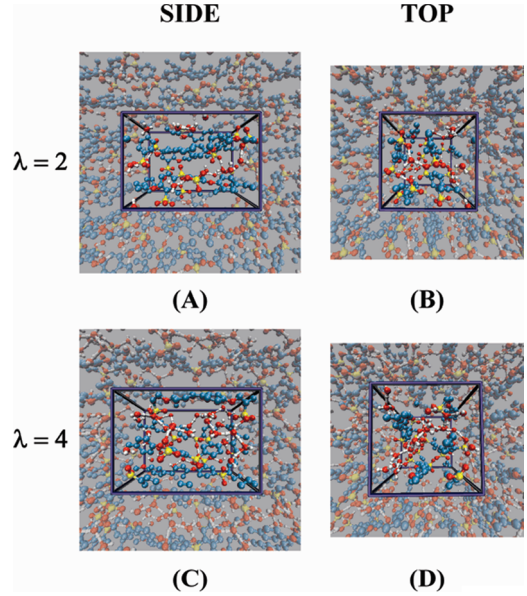

Figure 2. Snapshots of the configurations of $\lambda = 2$ (A and B) and $\lambda = 4$ (C and D). Atom types are denoted by color as follows: red, oxygen; white, deuterium; cyan, carbon; yellow, sulfur. For clarity, deuterium atoms attached to carbon atoms are omitted. Some equivalent atoms located outside the unit cell (shown by rectangles or squares) are also shown.

TABLE 1: Simulation Conditions for Hydrated SPES

	condition	
	λ ($(N_{D_2O} + N_{D_3O^+})/N_{SO_3^-}$) = 2	$\lambda = 4$
Number of Molecules in a Unit Cell		
N_{SPES}	4	4
N_{D_2O}	8	24
$N_{D_3O^+} = N_{SO_3^-}$	8	8
Size of Unit Cell		
x/Å	18.920	19.800
y/Å	13.244	13.860
z/Å	13.244	13.860

The model for SPES used in the cluster calculation is also depicted in Figure 1 along with a model system for Nafion, which is identical to the model that Glezakou et al. employed in their cluster solvation study.[22] We constructed the model hydration system for $RSO_3H + (H_2O)_n$ ($n = 2-4$). Geometry optimizations were carried out with density functional theory (DFT)[50,51] employing the B3LYP hybrid functional.[52,53] The 6-311++G(2d,2p) Gaussian basis sets were used for all of the atoms.[54] As demonstrated by computational studies on sulfuric acid−water clusters,[55,56] this level of basis set is necessary to correctly describe the S−O bond; basis sets smaller than this level give rise to a longer S−O bond.[57] All of the quantum chemical calculations were carried out using the Gaussian 03 program package.[58]

B. First-Principles MD Simulations. Snapshots of configurations from the first-principles MD simulations are presented in Figure 2. Details of the simulation conditions are contained in Table 1. SPES at low hydration was modeled by four SPES units and surrounding water molecules in a supercell (Figure 2), each unit of which contained one SO_2 and two sulfonic groups, as shown in Figure 1a. The size of the supercell was chosen to reproduce the experimental density of dry SPES membrane and bulk water at 353 K for the two hydration levels given in Table 1. In both simulations, the system was first equilibrated at high temperatures (above 1000 K), followed by

annealing to the target temperature in 40 ps, during which period all intramolecular covalent bond lengths were kept fixed with the RATTLE algorithm[59] to avoid dissociation. Then, all constraints on the bond lengths were removed, and after a further equilibration period of 6 ps, statistics were collected during the production run of 20 ps. The temperature was controlled by the Berendsen thermostat[60,61] with a target temperature of 353 K. During the first-principles MD simulations, the electronic structures of the systems were evaluated by means of DFT in the Kohn−Sham formalism with the Perdew−Burke−Ernzerhof (PBE) functional,[62] which is expected to give an accurate description of the hydrogen bonds.[63,64] For example, Truhlar et al. carried out extensive benchmark tests for various functionals available and concluded that the best performers for hydrogen bonding are PBE, PBE1PBE, B3P86, MPW1K, B97-1, and X3LYP.[63] Also, Bieckelhaupt et al. investigated the performance of density functionals for the hydrogen bonds in DNA base pairs. According to the results of Bieckelhaupt et al., the performance of PBE is better than other GGA type functionals such as BLYP.[64] Separable norm-conserving pseudopotentials[65−67] were employed, and only the Γ point was used to sample the Brillouin zone. Adaptive finite elements[68,69] were used in place of ordinary plane waves for the basis set. All production runs in the present paper were performed with an average cutoff energy of 45−50 Ry, while the resolution was approximately doubled at the positions of the oxygen and carbon atoms by adaptation of the grids.[70] In the molecular dynamics part, the nuclei were treated classically, and their equations of motion were integrated using the velocity-Verlet algorithm with the forces calculated from the electronic structure. All hydrogen atoms in the system were given the mass of deuterium to allow the use of a large time step of 1.21 fs in the production run. Below, in discussing dynamical properties, to avoid confusion, we explicitly denote deuterium. The electronic states were quenched to the Born−Oppenheimer surface at every time step with the limited-memory variant of the quasi-Newton method.[71−74] The wave functions were extrapolated from previous time steps.[75]

All of the first-principles MD simulations were carried out with our own finite element DFT code *FEMTECK* (Finite Element Method-based Total Energy Calculation Kit).

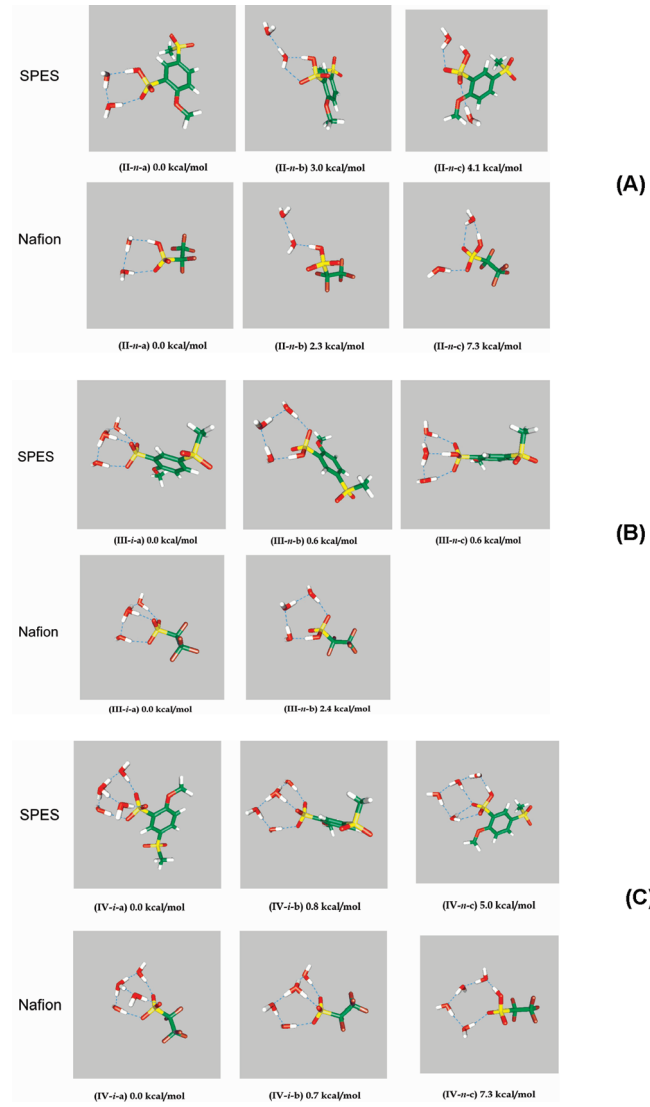

Figure 3. (A) The three lowest-energy structures for dihydrates of model SPES and Nafion. Fluorine atoms are depicted in purple. (B) Various isomeric structures for trihydrates of model SPES and Nafion. (C) Various isomeric structures for tetrahydrates of model SPES and Nafion.

III. Results and Discussion

A. Microsolvation of Model Clusters. We first compare the energetics of microsolvated clusters of the model Nafion and SPES. Figure 3A shows optimized structures of various dihydrated complexes of the model Nafion and SPES. We classify the isomeric forms of several clusters using the following notation: (III-*i*-a), where III indicates trihydrate, *i* or *n* denotes ionic or neutral clusters, and a, b, ... indicate a first, second, etc., isomeric form. It is seen in Figure 3A that an isomer where a water dimer forms a hydrogen-bonded cyclic structure is lowest in energy for both Nafion and SPES. This is in agreement with results of a previous similar modeling study by Paddison et al.[44] A linear hydrogen-bonded isomer is calculated to be the second lowest isomer, and an isomer where each S═O or S−OH is hydrogen bonded by a single water molecule is calculated to be higher in energy than the two other isomers. As already pointed out by Paddison et al., two water molecules are not enough to dissociate a proton from the sulfonic groups.[44] Figure 3B shows various isomers of trihydrates. It is seen that an ionic isomer where a proton is transferred from the sulfonic groups to a neighboring water molecule is lowest in energy for both Nafion and SPES. In the case of the model Nafion, the neutral hydrate (III-*n*-b) is computed to be 2.4 kcal/mol higher in energy than the ionic hydrate, while, in the case of the model SPES, the difference between the neutral and ionic conformers is only 0.6 kcal/mol. The energy difference between the ionic and neutral isomers is obviously larger in Nafion than in SPES. In the SPES trihydrate, there is a neutral isomer that closely resembles the (III-*i*-a) isomer in which the proton is not transferred to a neighboring water molecule. We were not able to obtain such an isomer for Nafion trihydrate. These results imply that Nafion tends to favor ionic isomers when hydrated by three water molecules, while, as the small energy difference between the ionic and neutral isomers indicates, we could not observe such a noticeable difference in the case of SPES trihydrate. For tetrahydrated isomers, the stability of an ionic isomer becomes greater than in the trihydrate case, as seen in Figure 3C. For Nafion tetrahydrates, the ionic isomer is computed to be 7.3 kcal/mol more stable than the neutral isomer. This trend is also observed in the case of SPES tetrahydrates, in which the ionic isomer is computed to be 5.0 kcal/mol more stable than a neutral isomer. In our computations, the isomer (IV-*i*-a), which corresponds to a solvent-separated ion pair, is computed to be more stable than the isomer (IV-*i*-b), which

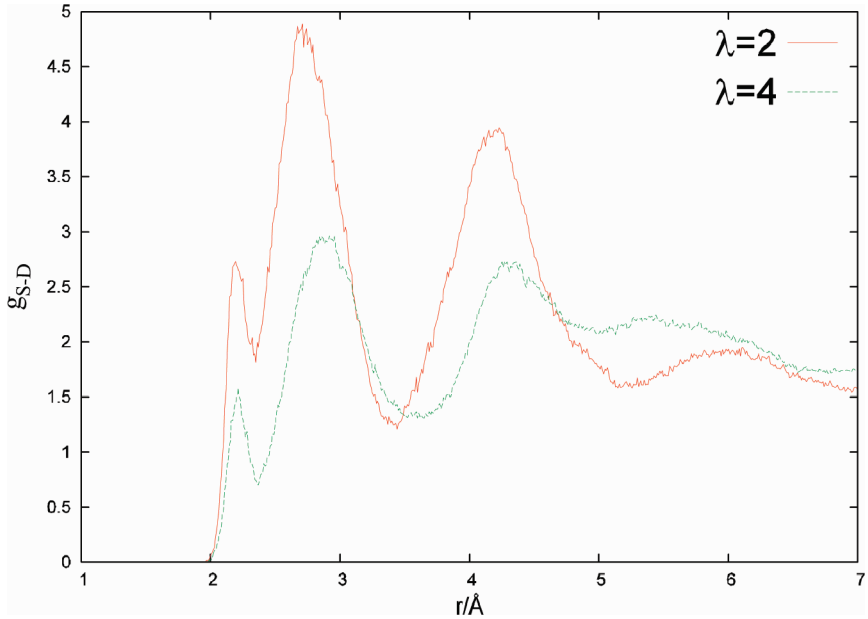

Figure 4. RDFs for an atomic pair between the sulfur atom of SO_3 and deuterium atoms. Deuterium atoms attached to carbon atoms are excluded from the calculation of RDFs.

represents a contact ion pair. This result differs from the results of the previous study in which it was reported that the isomer (IV-*i*-b) is the lowest energy isomer.[44] However, the energy difference between (IV-*i*-a) and (IV-*i*-b) is very small for both SPES and Nafion, which indicates that isomerization from (IV-*i*-b, contact ion pair) to (IV-*i*-a, solvent-separated ion pair) can occur easily.

For the tri- or tetrahydrates, the energy difference between the ionic and neutral isomers is always larger in the model Nafion than in the model SPES. Thus, the results suggest that the sulfonic groups of Nafion are more acidic than those of SPES. However, at the same time, it can be inferred from the results that, for SPES, four water molecules are enough to dissociate a proton from the sulfonic groups. Moreover, the results show that, because for SPES tetrahydrate the difference in energetics of the solvent-separated pair and the contact ion pair is very small, the dissociated proton can be easily transported from a location where it forms a contact ion pair to a position where it forms a solvent-separated ion pair. Therefore, just considering the microsolvation, although the energy difference between the ionic and neutral isomers is larger in Nafion than in SPES, it seems likely that the proton conductivity of Nafion and SPES at a low hydration level may not differ greatly.

B. Dynamical Simulations. Having discussed the features of energetics of the model hydrated clusters, we now discuss results obtained from the first-principles MD simulations. In Figure 4, radial distribution functions (RDFs) between the sulfur atom of SO_3^- and deuterium atoms are presented. The peak located around 2.2 Å results from an atomic pair between the deuterium atom in $-SO_3D$ and sulfur atoms of the sulfonic groups, which indicates that not all protons are dissociated from the sulfonic groups for both hydration levels. Integration of this peak located around 2.2 Å results in values of 0.21 and 0.24 for $\lambda = 2$ to $\lambda = 4$, respectively, where λ is defined as the number of water molecules per sulfonic group. These values should be zero if protons in the sulfonic groups are fully dissociated from it. The second peak of the RDFs shown in Figure 4 arises from hydrogen bonds between $-SO_3^-$ and water molecules. The results on the microsolvation demonstrate that, for dihydrates, which are closely related to $\lambda = 2$, a neutral isomer is energetically more favorable than an ionic isomer. However, in the first-principles MD simulations, some deuteriums in the sulfonic groups are dissociated even for $\lambda = 2$. To obtain insight into its origin, we investigated the time evolution of the number of water molecules that directly hydrate the sulfonic groups. In Figure 5, we present the number of water molecules around one of the sulfonic groups (panel A) as well as the average number of water molecules around all of the sulfonic groups (panel B). As shown in Figure 5, the number of water molecules around the sulfonic groups changes dynamically, ranging from one to four, during the simulations and an instantaneous increase of a local concentration of water molecules around the sulfonic groups is observed, which contributes to the dissociation of deuteriums even for $\lambda = 2$.

In Figure 6A, RDFs between the sulfur atom and O_w, where O_w denotes the oxygen atom of water molecules or hydronium ions, are presented. It is seen that the RDF is less structured in $\lambda = 4$ and also it can be inferred that a large portion of water molecules for $\lambda = 2$ is localized within the first hydration shell. As demonstrated by previous modeling studies, such a feature is also observed in hydrated Nafion.[34] The number of water molecules that directly hydrate the sulfonic groups, which is calculated by integrating the RDFs, is 2.2 for $\lambda = 2$ and 3.0 for $\lambda = 4$. In $\lambda = 4$, there are, on average, only three water molecules around the sulfonic groups, which gives rise to the incomplete deprotonation of the sulfonic groups.

RDFs for an atomic pair between O_w are presented in Figure 6B. The number of water molecules located within the first hydration shell is 1.2 and 2.0 for $\lambda = 2$ and $\lambda = 4$, respectively. Such small coordination numbers indicate that, for both hydration levels, the state of the water molecules is far from being bulk-like because the water molecules are not tetra-coordinated. To further investigate the water hydrogen-bond topology, we carried out a cluster analysis, with the results being shown in Figure 7. In the cluster analysis, a hydrogen bond was said to be present if the O···H bond length was less than 2.0 Å. In this analysis, we identified clusters of water molecules connected by a hydrogen-bond network in all snapshots. The number of water molecules in each cluster was then extracted, and the average population of each size of cluster was calculated. The

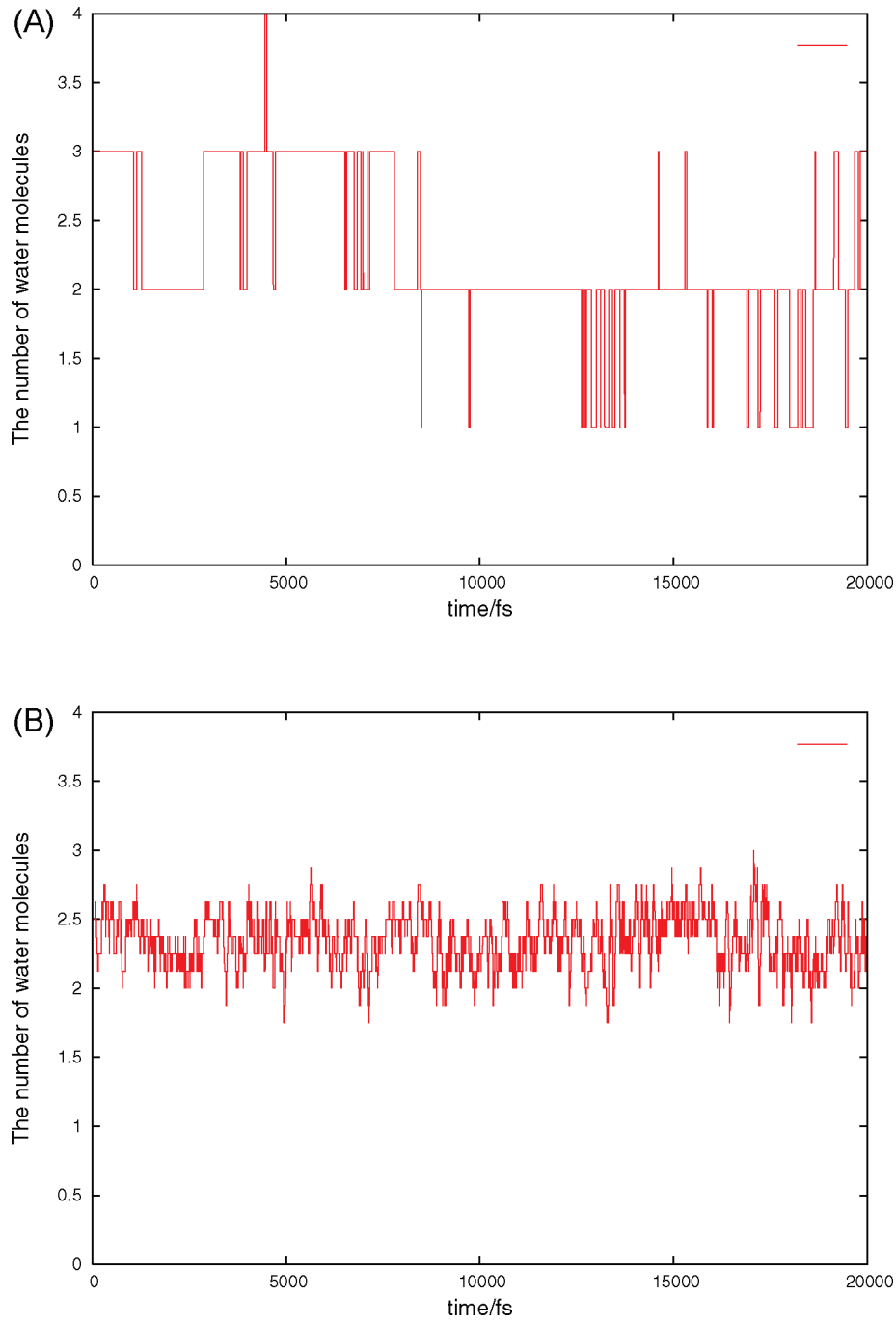

Figure 5. (A) Time evolution of the number of water molecules around one of the sulfonic groups. (B) Time evolution of the average number of water molecules around all sulfonic groups.

cluster size distribution stands for the average number of water clusters present in the system that corresponds to a particular cluster size.[76] For $\lambda = 2$, as shown in Figure 7, the population of water clusters whose size is larger than six is zero. For $\lambda = 2$, there is a significant contribution of cluster size four to the population. It is seen in Figure 7 that large water clusters are more abundant for $\lambda = 4$ than for $\lambda = 2$. The distribution of water cluster sizes for $\lambda = 4$ is very similar to the distribution in Nafion, whose hydration level is $\lambda = 4.25$,[77] allowing connection between water molecules hydrating SO_3^- and water molecules hydrating SO_2 through hydrogen bonds. Figure 8 shows RDFs between the sulfur atom of SO_2 and O_w. It is seen that the first peak that results from hydrogen bonds between SO_2 and water molecules is more structured in the case of $\lambda = 2$ than in the corresponding peak for $\lambda = 4$. This result indicates that water molecules participating in the solvation of SO_2 are rather immobile in the case of $\lambda = 2$ compared with the corresponding water molecules for $\lambda = 4$, which, in conjunction with the results on the cluster analysis, leads to the interpretation that, because for $\lambda = 4$ water molecules around SO_2 and SO_3^- are connected by hydrogen bonds, frequent exchanges of water molecules around SO_2 with other water molecules are permitted, while, in the case of $\lambda = 2$, such an exchange is rather unlikely.

We now discuss how the above differences in the hydrogen-bond network structure of water affect the proton diffusion in SPES. To calculate the diffusion coefficients of the protonic defects (hydronium ion) and the water molecules, we used the Einstein relation $D = \lim_{\tau\to\infty}(1/6\tau)\langle|\vec{r}_i(\tau) - \vec{r}_i(0)|\rangle^2$, where $\vec{r}_i(\tau)$ is the position of atom i, τ is a time interval, and $\langle x\rangle$ represents the ensemble average of a quantity x. The time evolution of

the mean square displacement (MSD) of O_w and D_w, where D_w denotes deuterium atoms of water molecules or hydronium ions, is presented in Figure 9. The computed diffusion coefficients for O_w are 0.24×10^{-5} and 0.32×10^{-5} cm^2/s for $\lambda = 2$ and $\lambda = 4$, respectively. The values are slightly different, although the comparison may only be meaningful within a qualitative sense because of statistical errors. As seen in the figure, all four MSD profiles exhibit very similar features, especially after 8 ps. If the excess deuteriums diffuse much more effectively than water molecules do, the slope of D_w's MSD should be steeper than that of O_w. Because the MSDs show a very similar profile, such a result indicates that the effective proton transport machinery is not functioning for $\lambda = 2$ and $\lambda = 4$. For the diffusion of the protonic defect, we were not able to obtain meaningful statistics, especially for $\lambda = 2$. Qualitatively, diffusion coefficients of deuteriums (not shown) for both hydration levels are computed to be identical.

To further probe the dynamical aspects of the deuteriums, we have computed a time correlation function, which is defined as

$$C_p(\tau) = \frac{\langle h_i(\tau) \cdot h_i(0) \rangle}{\langle h_i \rangle} \quad (1)$$

where $h_i(\tau)$ is unity if an oxygen atom i is coordinated by three hydrogen atoms and zero otherwise.[78−80] The function represents the conditional probability that the excess deuterium located at oxygen i at time 0 retains its identity at a time τ later.[78] Features of the function for both hydration levels shown in Figure 10 are very similar, indicating the similarity of proton transfer kinetics for both hydration levels. As shown in Figure 9, the function shows fast decays during the first few picoseconds and then decays very slowly at longer times. The rapid decay of the function means that a

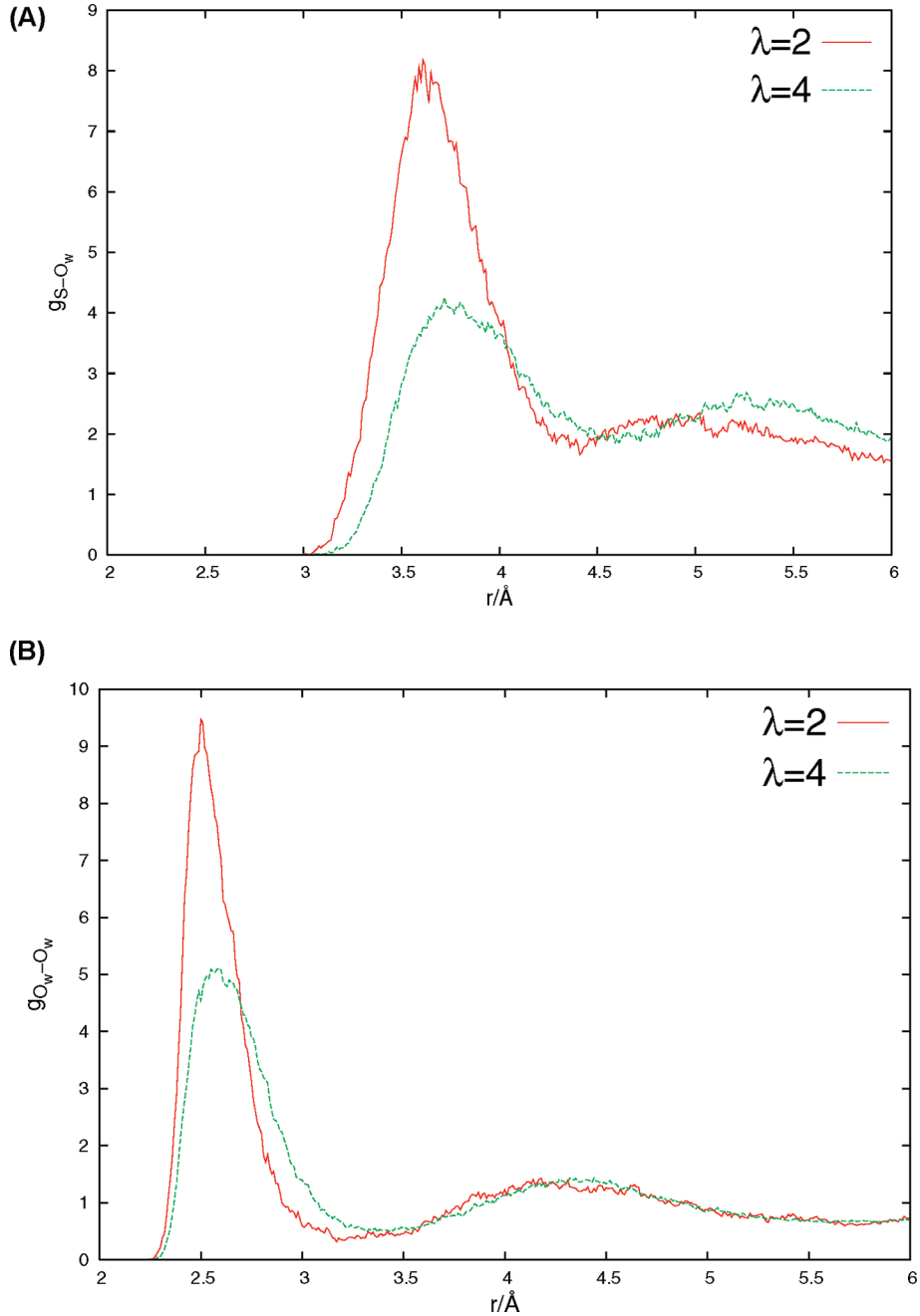

Figure 6. (A) RDFs for an atomic pair between the sulfur atom of SO_3 and O_w, where O_w denotes oxygen atoms of water molecules or hydronium ions. (B) RDFs for a pair of O_w.

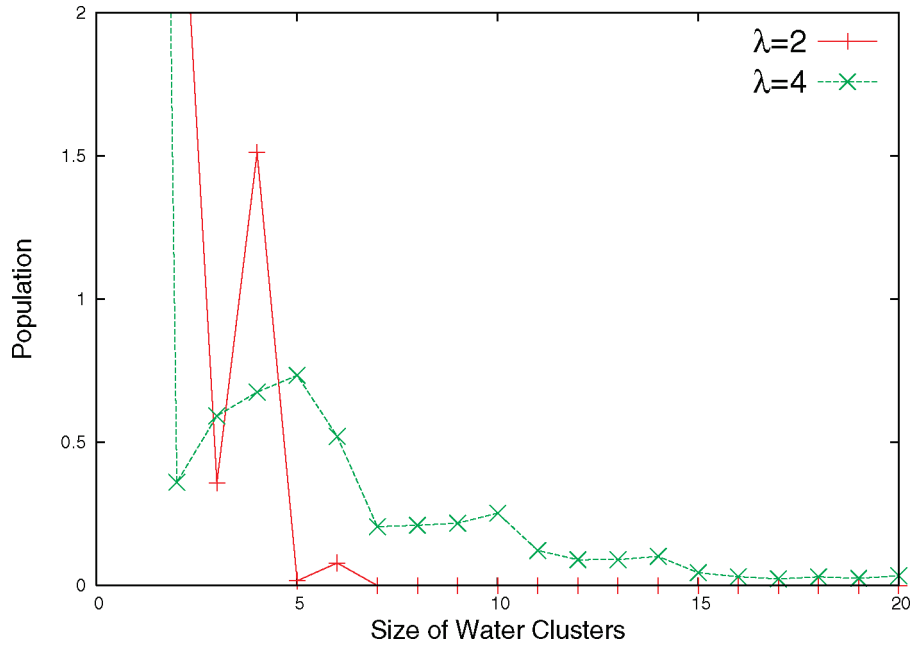

Figure 7. Results of cluster analysis.

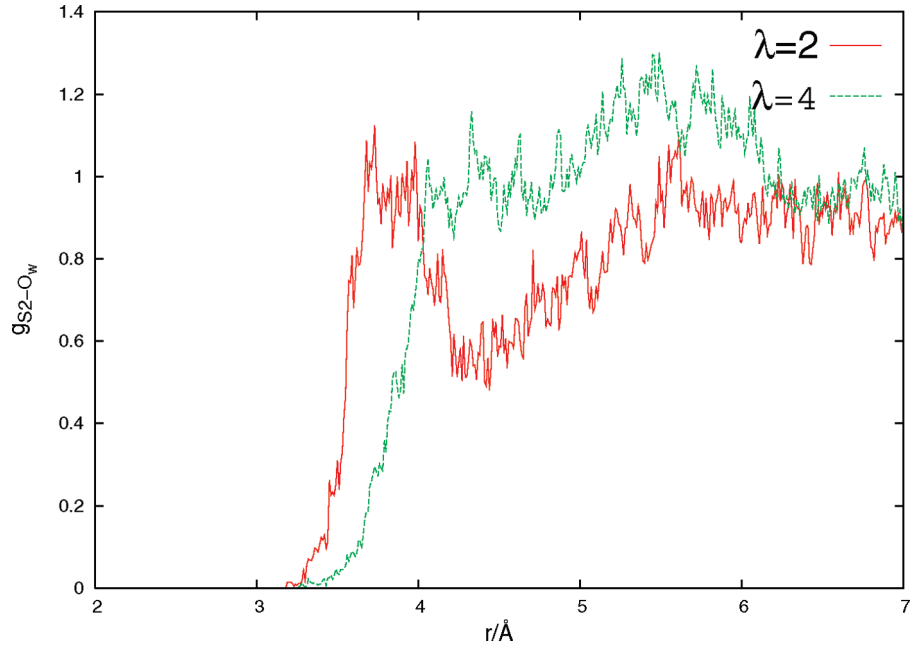

Figure 8. RDFs for an atomic pair between the sulfur atom of SO_2 and O_w. S2 indicates the sulfur atom of SO_2.

hydronium ion transfers its excess proton to a neighboring water molecule within a very short period. The same analysis applied to protons in water shows that the value of $C_p(\tau)$ drops to about 0.3 at $\tau = 10$ ps, while in the present systems, as seen in Figure 10, the corresponding value is about 0.6 at $\tau = 10$ ps. Such a slow decay of the functions indicates that a hydronium ion retains its identity for a longer time. To gain insights into the proton transfer details, we now introduce two types of proton transfer, details of which are described in our previous papers.[42,43] The *constructive* proton transfer is the transfer of a proton that moves farther away from its original position. On the other hand, the *nonconstructive* proton transfer is the transfer of a proton that returns to the position of the oxygen site of the original water in the end. The latter type of proton transfer occurs on a very short time scale, as already reported by several authors,[81,82] and can be described as an oscillatory motion of an excess proton between two water molecules. Therefore, the fast decay of the functions represents the *nonconstructive* proton transfer event. The overall picture of proton transfer in low-hydration SPES that can be inferred from the above analysis is that the protons are transported as a hydronium ion while the proton itself is oscillating in between two water molecules, a phenomenon that is also named by the term *special pair dance*.[82] Molecular dynamics simulations of hydrated Nafion utilizing a reactive force field for water show that proton transfer kinetics follows a second order reaction.[33] Hofmann et al. indicate that, since the lifetime of hydronium ion is shorter at higher water content, the decay of hydronium ions follows the second order kinetics. As shown in Figure 10, the features of the correlation functions for $\lambda = 2$ and $\lambda = 4$ are very similar. However, the correlation functions for $\lambda = 67.5$ show very rapid decay, indicating that the lifetime of hydronium ions in hydrated SPES ($\lambda = 67.5$)[83] is shorter

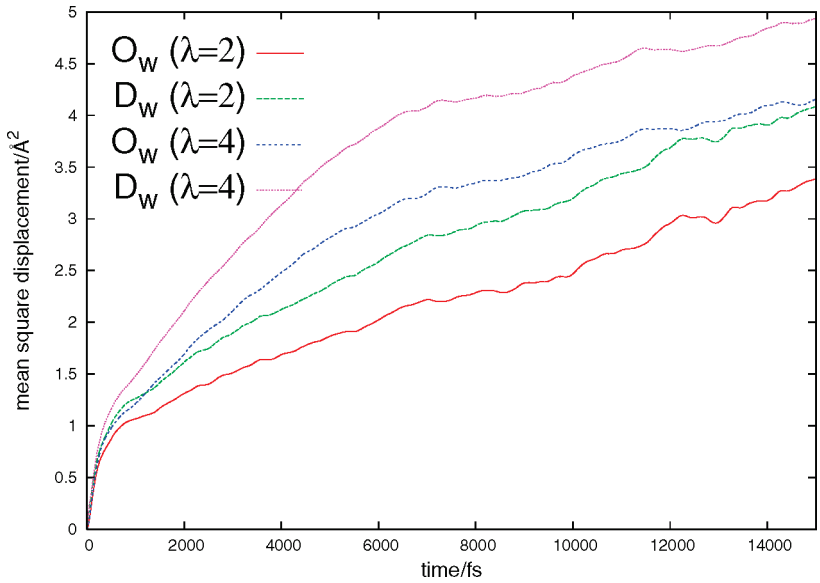

Figure 9. Time evolution of the MSD for D_w and O_w, where D_w is a deuterium atom of D_2, O, or D_3O^+.

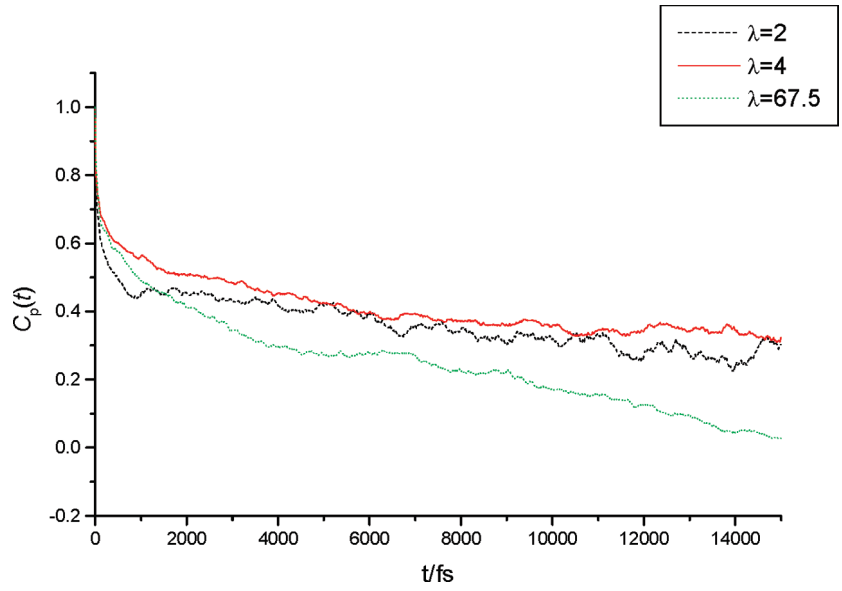

Figure 10. Plots of the time correlation function defined by eq 1.

than that of hydrated SPES (λ = 2, 4). The results imply that, as in the case of Nafion, the hydronium decay follows the second order kinetics.

According to the above analysis, the proton transport in low-hydration SPES occurs in a manner that is slow and less effective than highly hydrated ones. As the results of the cluster analysis show, the hydrogen-bond network of water molecules is significantly disconnected in low-hydration SPES. We can also understand the ineffective proton transport in such an environment from a previously proposed analysis on methanol−water mixtures.[84] Agmon et al. have explained the proton conductivity of the mixture employing "*the pathway model*" and "*the percolation model*". In both models, which are statistical models in nature, it is assumed that methanol molecules that are directly ligated to H_3O^+ (or $H_5O_2^+$) block the proton migration out of such structures. Hence, an increase in methanol molecules ligated to H_3O^+ (or $H_5O_2^+$) decreases the proton conductivity in the mixture. A similar argument can be applied to low-hydration SPES. Let us assume that a hydronium ion is fully hydrated. In such a case, migration of a proton located in the central hydronium ion to all other hydrating water molecules is allowed. However, when a hydronium ion is not fully hydrated, migration of a proton from the central hydronium ion to the vacant site where there is no water molecule that directly hydrates is prohibited, leading to the reduction of proton mobility as the increase of ligation of methanol to a hydronium ion reduces the proton mobility. Hence, the disconnected hydrogen-bond network of water molecules in low-hydration SPES results in ineffective proton transport.

IV. Discussion

As demonstrated by the quantum chemical calculations on the microsolvated clusters of the model compounds, protons of the sulfonic groups are more acidic in Nafion than in SPES. The results of the computations indicate that, in the case of Nafion, the sulfonic groups can release protons upon solvation by three water molecules because the energy difference between the ionic and neutral isomers is large (the ionic isomer is lower in energy). With solvation by four water molecules, the sulfonic groups of both SPES and Nafion can release protons. Such a

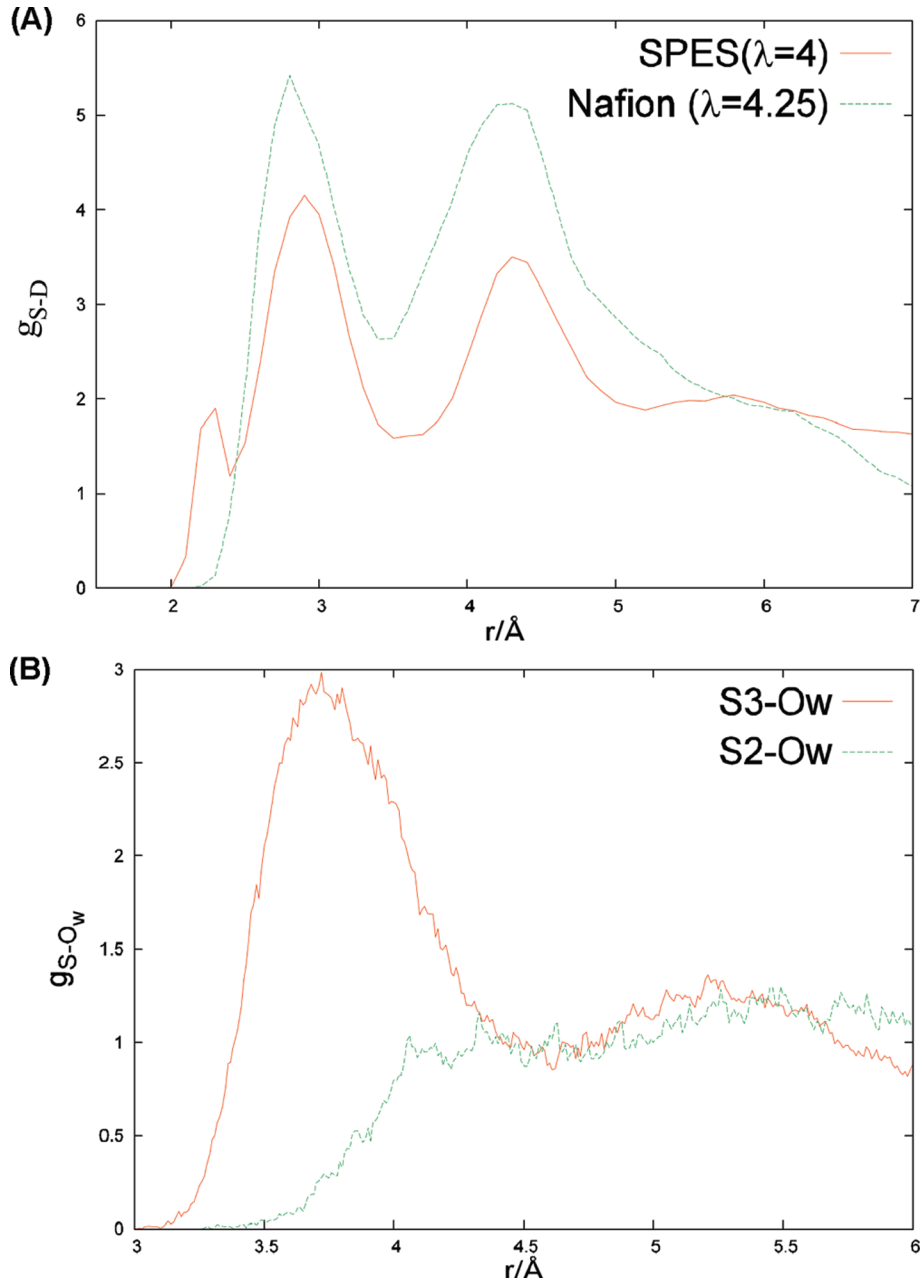

Figure 11. (A) Comparison of RDFs between the sulfur of SO_3^- and D_w of SPES ($\lambda = 4$) and Nafion ($\lambda = 4.25$). (B) Comparison of RDFs. The red line indicates the RDF between the sulfur atom of SO_3 and O_w, and the green line indicates the RDF for an atomic pair between the sulfur atom of SO_2 and O_w for $\lambda = 4$.

result implies that, while the acidity of the sulfonic groups between Nafion and SPES differs to some extent, if the sulfonic groups of SPES or Nafion are fully solvated by at least four water molecules, the dissociation of a proton from the sulfonic groups can occur with ease. RDFs for an atomic pair between S and D atoms for SPES ($\lambda = 4$) and Nafion ($\lambda = 4.25$) are compared in Figure 11A. As seen in the figure, while the hydration levels for SPES and Nafion are slightly different, a peak located around 2.2 Å is not observed in Nafion, which indicates that deuteriums are completely dissociated from the sulfonic groups. The number of water molecules around the sulfonic groups is 3.2 and 4.1 for SPES and Nafion, respectively. The results imply that, in the case of Nafion, water molecules are hydrating the sulfonic groups in a manner that is effective for the dissociation of protons. This difference in the hydration environment around the sulfonic groups between SPES and Nafion may stem from the difference in the native chemical structure of both membranes. As seen in Figure 1, the backbone of SPES contains SO_2 groups. Figure 11B shows RDFs between the sulfur atoms of SO_3^- or SO_2 and O_w for SPES ($\lambda = 4$). As seen in the RDFs, while hydration around the SO_2 is weak compared with that around SO_3^-, it is clear that some water molecules participate in hydrating SO_2, which means that some water molecules are used up for the solvation of SO_2 rather than for the hydration of SO_3^- (roughly three water molecules hydrate SO_3^- and one water molecule hydrates SO_2). When the water content is high, such a hydration pattern is not problematic because there are enough water molecules to fully hydrate SO_3^- and SO_2. However, when the water content is low, such an environment gives rise to insufficient hydration around SO_3^-, leading to the partial deprotonation of the sulfonic groups, and may affect the overall performance of the PEFC.

Considering the above discussion, it is possible to suggest that, for effective proton transport in low-hydration SPES,

removal of SO_2 functional groups or replacement of SO_2 by other hydrophobic groups is beneficial for the improvement of proton conductivity of the membranes. In addition, introduction of a bulky substituent around SO_2, which is expected to prevent access of water molecules to SO_2, may be useful. Such a treatment is expected to enhance local hydration around SO_3^- and increase the connectivity of the water hydrogen-bond network, while more elaborate results may be obtained from molecular simulations employing model systems larger than those employed in the present study.

V. Conclusion

In the present study, properties of SPES were investigated theoretically by means of several computational modeling techniques and compared with those of Nafion. Quantum chemical calculations on microsolvated clusters show that, up to solvation by two water molecules, a neutral isomer is more stable than an ionic isomer. With three water molecules, an ionic isomer is computed to be more stable than a neutral isomer for both Nafion and SPES, although the energy difference between the two isomers is very small in the case of SPES. Hydration by four water molecules allows the dissociation of protons from the sulfonic groups for both Nafion and SPES. The energy difference between an ionic and neutral isomer is computed to be always larger for Nafion than for SPES.

Further details of the proton dynamics are obtained from the first-principles MD simulations. We could not observe a significant difference in proton dynamics for both hydration levels ($\lambda = 2, 4$). The dynamics of protons in low-hydration SPES is contributed mostly from the short-scale proton dynamics, which can be described as oscillatory motions of an excess proton between two water molecules.

Compared with low-hydration Nafion, protons are not completely dissociated from the sulfonic groups in low-hydration SPES. Such a result stems from insufficient solvation around the sulfonic groups. The results of simulations show that SO_2 groups have a negative effect that hinders effective hydrations around SO_3. Therefore, removal of SO_2 groups is expected to enhance the performance of PEFCs employing SPES as a PEM to a certain degree.

Finally, we mention that, since all of the first-principles MD simulations were carried out using deuterium atoms instead of hydrogen atoms, the conclusion needs some considerations about the transferability of the results from heavy water to water, especially for the dynamical properties.[85]

Acknowledgment. All of the computations were carried out at AIST Super Cluster, the high performance computing facility at FC-Cubic and the T2K system at the University of Tokyo. This study was supported in part by a Grant-in-Aid for Scientific Research on Priority Areas "Molecular Theory for Real Systems" from the Ministry of Education, Culture, Sports, Science, and Technology, Japan, by the Ministry of Economy, Trade, and Industry (METI), Japan, and the New Energy and Industrial Technology Development Organization (NEDO), Japan.

Supporting Information Available: Energetics, Cartesian coordinates, and Mulliken charges of isomers shown in Figure 3 and comparison of mean square displacement. This material is available free of charge via the Internet at http://pubs.acs.org.

References and Notes

(1) Steele, B. C. H.; Heinzel, A. *Nature* **2001**, *414*, 315.
(2) Prater, K. B. *J. Power Sources* **1996**, *61*, 105.
(3) Hamrock, S. J.; Yandrasits, M. A. *J. Macromol. Sci., Part C: Polym. Rev.* **2006**, *46*, 219.
(4) Mauritz, K. A.; Moore, R. B. *Chem. Rev.* **2004**, *104*, 4535.
(5) Hickner, M. A.; Ghassemi, H.; Kim, Y. S.; Einsla, B. R.; McGrath, J. E. *Chem. Rev.* **2004**, *104*, 4587.
(6) Dai, H.; Guan, R.; Li, C.; Liu, J. *Solid State Ionics* **2007**, *178*, 339.
(7) Hickner, M. A.; Fujimoto, C. H.; Cornelius, C. J. *Polymer* **2006**, *47*, 4238.
(8) Smitha, B.; Sridhar, S.; Khan, A. A. *J. Membr. Sci.* **2005**, *259*, 10.
(9) Li, Q.; He, R.; Jensen, J. O.; Bjerrum, N. J. *Chem. Mater.* **2003**, *15*, 4896.
(10) Carretta, N.; Tricoli, V.; Picchioni, F. *J. Membr. Sci.* **2000**, *166*, 189.
(11) Lufrano, F.; Squadrito, G.; Patti, A.; Passalacqua, E. *J. Appl. Polym. Sci.* **2000**, *77*, 1250.
(12) Kim, H.-J.; Krishnan, N. N.; Lee, S.-Y.; Hwang, S. Y.; Kim, D.; Jeong, K. J.; Lee, J. K.; Cho, E.; Lee, J.; Han, J.; Ha, H. Y.; Lim, T.-H. *J. Power Sources* **2006**, *160*, 353.
(13) Kreuer, K. D. *J. Membr. Sci.* **2001**, *185*, 29.
(14) Norsten, T. B.; Guiver, M. D.; Murphy, J.; Astill, T.; Navessin, T.; Holdcroft, S.; Frankamp, B. L.; Rotello, V. M.; Ding, J. *Adv. Funct. Mater.* **2006**, *16*, 1814.
(15) Ghassemi, H.; Subbaraman, R.; Brockman, C.; Pyle, B.; Zawodzinski, T., Jr. http://www.electrochem.org/meetings/scheduler/abstracts/214/0857.pdf
(16) Kreuer, K. D. *Solid State Ionics* **1997**, *97*, 1.
(17) http://en.wikipedia.org/wiki/Nafion#cite_note-5 (accessed Sept 17, 2009).
(18) Scharfenberger, G.; Meyer, W. H.; Wegner, G.; Schuster, M.; Kreuer, K.-D.; Maier, J. *Fuel Cells* **2006**, *6*, 237.
(19) Nguyen, T. V.; Knobbe, M. W. *J. Power Sources* **2003**, *114*, 70.
(20) Davanathan, R. *Energy Environ. Sci.* **2008**, *101*, 101.
(21) Elliot, J. A.; Paddison, J. *Phys. Chem. Chem. Phys.* **2007**, *9*, 2602.
(22) Glezakou, V.-A.; Dupuis, M.; Mundy, C. J. *Phys. Chem. Chem. Phys.* **2007**, *9*, 5752.
(23) Marx, D.; Tuckerman, M. E.; Hutter, J.; Parrinello, M. *Nature* **1999**, *397*, 601.
(24) Marx, D. *ChemPhysChem* **2006**, *7*, 1848.
(25) Boero, M.; Ikeshoji, T.; Terakura, K. *ChemPhysChem* **2005**, *6*, 1775.
(26) Chandra, A.; Tuckerman, M. E.; Marx, D. *Phys. Rev. Lett.* **2007**, *99*, 145901.
(27) Petersen, M. K.; Wang, F.; Blake, N. P.; Metiu, H.; Voth, G. A. *J. Phys. Chem. B* **2005**, *109*, 3727.
(28) Petersen, M. K.; Voth, G. A. *J. Phys. Chem. B* **2006**, *110*, 18594.
(29) Petersen, M. K.; Hatt, A. J.; Voth, G. A. *J. Phys. Chem. B* **2008**, *112*, 7754.
(30) Dokmaisrijan, S.; Spohr, E. *J. Mol. Liq.* **2006**, *129*, 92.
(31) Seeliger, D.; Hartnig, C.; Spohr, E. *Electrochim. Acta* **2005**, *50*, 4234.
(32) Spohr, E.; Commer, P.; Kornyshev, A. A. *J. Phys. Chem. B* **2002**, *106*, 10560.
(33) Hofmann, D. W. M.; Kuleshova, L.; D'Aguanno, B. *J. Mol. Model.* **2008**, *14*, 225.
(34) Devanathan, R.; Venkatnathan, A.; Dupuis, M. *J. Phys. Chem. B* **2007**, *111*, 13006.
(35) Devanathan, R.; Venkatnathan, A.; Dupuis, M. *J. Phys. Chem. B* **2007**, *111*, 8069.
(36) Venkatnathan, A.; Devanathan, R.; Dupuis, M. *J. Phys. Chem. B* **2007**, *111*, 7234.
(37) Lafitte, B. Proton-conducting sulfonated and phophonated polymers and fuel cell membranes by chemical modification of polysulfones. Doctoral Thesis, Lund University, 1997.
(38) Tsuchida, E. *J. Chem. Phys.* **2004**, *121*, 4740.
(39) Tsuchida, E. *J. Phys. Soc. Jpn.* **2006**, *75*, 054801.
(40) Choe, Y.-K.; Tsuchida, E.; Ikeshoji, T. *J. Chem. Phys.* **2007**, *126*, 154510.
(41) Choe, Y.-K.; Tsuchida, E.; Ikeshoji, T. *Comput. Phys. Commun.* **2007**, *177*, 38.
(42) Choe, Y.-K.; Tsuchida, E.; Ikeshoji, T.; Yamakawa, S.; Hyodo, S. *J. Phys. Chem. B* **2008**, *112*, 11586.
(43) Choe, Y.-K.; Tsuchida, E.; Ikeshoji, T.; Yamakawa, S.; Hyodo, S. *Phys. Chem. Chem. Phys.* **2009**, *11*, 3892.
(44) Eikerling, M.; Paddison, S. J.; Zawodzinski, T. A., Jr. *J. New Mater. Electrochem. Syst.* **2002**, *5*, 15.
(45) Paddison, S. J. *J. New Mater. Electrochem. Syst.* **2001**, *4*, 197.
(46) Paddison, S. J.; Elliott, J. A. *J. Phys. Chem. A* **2005**, *109*, 7583.
(47) Paddison, S. J.; Elliott, J. A. *Solid State Ionics* **2006**, *177*, 2385.
(48) Paddison, S. J.; Elliott, J. A. *Phys. Chem. Chem. Phys.* **2006**, *8*, 2193.
(49) Paddison, S. J.; Kreuer, K. D.; Maier, J. *Phys. Chem. Chem. Phys.* **2006**, *8*, 4530.

(50) Hohenberg, P.; Kohn, W. *Phys. Rev.* **1964**, *136*, B864.
(51) Kohn, W.; Sham, L. J. *Phys. Rev.* **1965**, *140*, A1133.
(52) Becke, A. D. *J. Chem. Phys.* **1993**, *98*, 5648.
(53) Lee, C.; Yang, W.; Parr, R. G. *Phys. Rev. B* **1988**, *37*, 785.
(54) Krishnan, R.; Binkley, J. S.; Seeger, R.; Pople, J. A. *J. Chem. Phys.* **1980**, *72*, 650.
(55) Choe, Y.-K.; Tsuchida, E.; Ikeshoji, T. *Int. J. Quantum Chem.* **2009**, *109*, 1984.
(56) Hintze, P. E.; Kjaergaard, H. G.; Vaida, V.; Burkholder, J. B. *J. Phys. Chem. A* **2003**, *107*, 1112.
(57) Re, S.; Osamura, Y.; Morokuma, K. *J. Phys. Chem. A* **1999**, *103*, 3535.
(58) Frisch, M. J.; Trucks, G. W.; Schlegel, H. B.; Scuseria, G. E.; Robb, M. A.; Cheeseman, J. R.; Montgomery, J. A., Jr.; Vreven, T.; Kudin, K. N.; Burant, J. C.; Millam, J. M.; Iyengar, S. S.; Tomasi, J.; Barone, V.; Mennucci, B.; Cossi, M.; Scalmani, G.; Rega, N.; Petersson, G. A.; Nakatsuji, H.; Hada, M.; Ehara, M.; Toyota, K.; Fukuda, R.; Hasegawa, J.; Ishida, M.; Nakajima, T.; Honda, Y.; Kitao, O.; Nakai, H.; Klene, M.; Li, X.; Knox, J. E.; Hratchian, H. P.; Cross, J. B.; Adamo, C.; Jaramillo, J.; Gomperts, R.; Stratmann, R. E.; Yazyev, O.; Austin, A. J.; Cammi, R.; Pomelli, C.; Ochterski, J. W.; Ayala, P. Y.; Morokuma, K.; Voth, G. A.; Salvador, P.; Dannenberg, J. J.; Zakrzewski, V. G.; Dapprich, S.; Daniels, A. D.; Strain, M. C.; Farkas, O.; Malick, D. K.; Rabuck, A. D.; Raghavachari, K.; Foresman, J. B.; Ortiz, J. V.; Cui, Q.; Baboul, A. G.; Clifford, S.; Cioslowski, J.; Stefanov, B. B.; Liu, G.; Liashenko, A.; Piskorz, P.; Komaromi, I.; Martin, R. L.; Fox, D. J.; Keith, T.; Al-Laham, M. A.; Peng, C. Y.; Nanayakkara, A.; Challacombe, M.; Gill, P. M. W.; Johnson, B.; Chen, W.; Wong, M. W.; Gonzalez, C.; Pople, J. A. *Gaussian 03*, revision E.01; Gaussian, Inc.: Wallingford, CT, 2004.
(59) Andersen, H. C. *J. Comput. Phys.* **1983**, *52*, 24.
(60) Berendsen, H. J. C.; Postma, J. P. M.; van Gunsteren, W. F.; DiNola, A.; Haak, J. R. *J. Chem. Phys.* **1984**, *81*, 3684.
(61) Morishita, T. *J. Chem. Phys.* **2000**, *113*, 2976.
(62) Perdew, J. P.; Burke, K.; Ernzerhof, M. *Phys. Rev. Lett.* **1996**, *77*, 3865.
(63) Truhlar, D. G.; Zhao, Y. *J. Chem. Theory Comput.* **2005**, *1*, 415.
(64) Wijst, T. v. d.; Guerra, C. F.; Swart, M.; Bickelhaupt, F. M. *Chem. Phys. Lett.* **2006**, *426*, 415.
(65) Kleinman, L.; Bylander, D. M. *Phys. Rev. Lett.* **1982**, *48*, 1425.
(66) Goedecker, S.; Teter, M.; Hutter, J. *Phys. Rev. B* **1996**, *54*, 1703.
(67) Hartwigsen, C.; Goedecker, S.; Hutter, J. *Phys. Rev. B* **1998**, *58*, 3641.
(68) Tsuchida, E.; Tsukada, M. *Phys. Rev. B* **1996**, *54*, 7602.
(69) Tsuchida, E.; Tsukada, M. *J. Phys. Soc. Jpn.* **1998**, *67*, 3844.
(70) Gygi, F. *Phys. Rev. B* **1995**, *51*, 11190.
(71) Press, W. H.; Teukolsky, S. A.; Vetterling, W. T.; Flannery, B. P. *Numerical Recipes in FORTRAN*; Cambridge University Press: Cambridge, U.K., 1992.
(72) Liu, D. C.; Nocedal, J. *Math. Prog.* **1989**, *45*, 503.
(73) Gill, P. E.; Leonard, M. W. *SIAM J. Optim.* **2003**, *14*, 380.
(74) Tsuchida, E. *J. Phys. Soc. Jpn.* **2002**, *71*, 197.
(75) Arias, T. A.; Payne, M. C.; Joannopoulos, J. D. *Phys. Rev. Lett.* **1992**, *69*, 1077.
(76) Cui, S.; Liu, J.; Selvan, M. E.; Paddison, S. J.; Keffer, D. J.; Edwards, B. J. *J. Phys. Chem. B* **2008**, *112*, 13273.
(77) For details, see ref 38.
(78) Köfinger, J.; Dellago, C. *J. Phys. Chem. B* **2008**, *112*, 2349.
(79) Vuilleumier, R.; Borgis, D. *J. Chem. Phys.* **1999**, *111*, 4251.
(80) In the actual calculation, eq 1 is modified in a manner to take into account the random recombination of a hydronium ion. The corrected time correlation function is as follows: probability = $C(0)/n_$oxygens (the number of oxygen), decay = $C(0) - C(t)$, correction = decay*probability, corrected = $C(t)$−correction*(1 + probability + probability**2 + probability**3).
(81) Morrone, J. A.; Haslinger, K. E.; Tuckerman, M. E. *J. Phys. Chem. B* **2006**, *110*, 3712.
(82) Markovitch, O.; Chen, H.; Izvekov, S.; Paesani, F.; Voth, G. A.; Agmon, N. *J. Phys. Chem. B* **2008**, *112*, 9456.
(83) Computational details on $\lambda = 67.5$ are reported elsewhere. See: Choe, Y.-K.; Tsuchida, E.; Ikeshoji, T.; Ohira, A.; Kidena, K. *ECS Trans.* **2009**, *25*, 1075.
(84) Agmon, N.; Goldberg, S. Y.; Huppert, D. *J. Mol. Liq.* **1995**, *64*, 161.
(85) Paesani, F.; Voth, G. A. *J. Phys. Chem. B* **2009**, *113*, 5702.

JP906757S